Available online at www.sciencedirect.com
ScienceDirect
Journal of Solid State Chemistry 181 (2008) 1314–1320
JOURNAL OF SOLID STATE CHEMISTRY
www.elsevier.com/locate/jssc

The $Sr_{2.75}Ce_{0.25}Co_2O_{7-\delta}$ oxide, $n = 2$ member of the Ruddlesden–Popper series: Structural and magnetic evolution depending on oxygen stoichiometry

A. Demont, S. Hébert, D. Pelloquin*, A. Maignan

Laboratoire CRISMAT, UMR 6508 CNRS ENSICAEN, 6 bd Maréchal Juin, 14050 CAEN Cedex 4, France

Received 3 August 2007; received in revised form 13 February 2008; accepted 14 February 2008
Available online 29 February 2008

Abstract

The second member of the Ruddlesden–Popper series, $n = 2$ in $Sr_{n+1}Co_nO_{3n+1}$, has been stabilized by substituting cerium for strontium leading to the pure compound $Sr_{2.75}Ce_{0.25}Co_2O_{7-\delta}$. The oxygen vacancies of this phase can be partially filled by a post-annealing oxidizing treatment with δ decreasing from 1.1 to 0.3 for the as-prepared and oxidized phases, respectively. As the samples are oxidized from $\delta \approx 1.1$ to 0.3, the a and b unit cell parameters decrease from 3.836 to 3.815 Å and from 20.453 to 20.047 Å, respectively. Despite the average value of the cobalt valence state, $V_{Co} \approx +3.5$, obtained in the oxidized $Sr_{2.75}Ce^{+4}_{0.25}Co_2O_{6.7}$ phase, a clear ferromagnetic state wit $T_C = 175$ K and $M_S = 0.8\,\mu B/Co$ is reached.

Keywords: Layered structure; Cobaltite; Ferromagnetism

1. Introduction

The strong orbital, charge and spin coupling in cobaltates make these oxides attractive for various physical properties such as spintronics [1], thermoelectricity [2] solid oxide fuel cells [3], superconductivity [4], quantum tunneling of the magnetization [5], metal to insulator transition [6], etc.

Among all the different charge and spin states for cobalt cations, the tetravalent cobalt cations in the structures derived from the perovskite, with corner-shared CoO_6 octahedra, favor a ferromagnetic metallic state. This is illustrated by $SrCoO_3$ ($T_C = 280$ K [7]) and Sr_2CoO_4 ($T_C = 270$ K [8]), $n = \infty$ and 1 members of the Ruddlesden–Popper (RP) series $Sr_{n+1}Co_nO_{3n+1}$, respectively. Nevertheless, this high oxidation state for cobalt requires specific chemical routes such as synthesis under high oxygen pressure [7], oxidation by electrochemistry [9] or thin-film techniques [8]. This difficulty is also illustrated by the lack of reports on the oxygen stoichiometric $n = 2$ RP phase. The structure of $Sr_3Co_2O_{7-\delta}$ is indeed obtained for large oxygen deficiency with δ values ranging from 0.94 to 1.62 [10,11], i.e. corresponding mainly to mixed Co^{2+}/Co^{3+} valency ($\delta = 1.62$, $V_{Co} = +2.38$) or to a slight amount of Co^{4+} in the Co^{3+} matrix ($\delta = 0.94$, $V_{Co} = +3.06$). In these phases, a large amount of oxygen vacancies are located at the level of the $SrO_{1-\delta'}$ central layer of the perovskite block, together with vacancies in the "$CoO_{n-\delta'}$" square planes mainly along one basal direction leading to a marked orthorhombic cell with $a \sim 3.9$ Å $\neq b \sim 3.7$ Å and $c \sim 20$ Å [10]. Remarkably, the most oxidized phases ($\delta \sim 1$) of $Sr_3Co_2O_{7-\delta}$ are very unstable in air showing a very rapid topotactic reaction with water inducing a c-axis expansion ($c \sim 28$ Å) due to the incorporation of hydroxide groups and water molecules at the level of the rocksalt-type layers $[Sr_2O_2]_\infty$ [12]. The strong air sensitivity of the $Sr_3Co_2O_{7-\delta}$ ($\delta \sim 1$) phases could originate from the unstable CoO_x polyhedra and thus, explaining the experimental difficulty to stabilize more oxidized phases such as $\delta \ll 1$. In the case of the $SrCoO_{3-\delta}$ perovskite ($n = \infty$ member of RP series), chemical substitutions on the Sr-site by rare-earth (or Y^{3+}) cations have been shown to be efficient to synthesize this phase [13,14]. Among the possible cations substituting for strontium, tetravalent cations such as Th^{4+}, ($n = \infty$) [9] or

*Corresponding author. Fax: +33 2 31 96 16 00.
E-mail address: pelloquin@ensicaen.fr (D. Pelloquin).

0022-4596/$ - see front matter © 2008 Elsevier Inc. All rights reserved.
doi:10.1016/j.jssc.2008.02.023

Ce^{4+} ($n = \infty$ [15,16] and $n = 1$ [17]) are also possible and allow also to create a sufficient Co^{4+} concentration for inducing ferromagnetism and metallicity in this perovskite structure.

In the following we report on the stabilization of the $Sr_{3-x}Ce_xCo_2O_{7-\delta}$ phase by substitution of Sr^{2+} by the Ce^{4+}. Despite the existence of a narrow domain of composition ($x \approx 0.25$) a ferromagnetic behavior has been induced by oxygen pressure post-annealing.

2. Experimental

The compounds $Sr_{3-x}Ce_xCo_2O_{7-\delta}$ have been prepared by mixing in a glove-box the precursors SrO, CeO_2 and Co_3O_4 according to the cations ratio $3-x$: x: $\frac{2}{3}$ with $x = 0.1$, 0.15, 0.2, 0.25, and 0.3. After pressing of the powder, bars (~1 g) were set in an alumina finger-like crucible, the latter being put in a silica ampoule. The closed ampoules, sealed under primary vacuum, were fired at 1200 °C for 12 h and then quenched in air. According to the starting oxygen content, summarized by the nominal $O_{5.66+x}$ stoichiometry, one expects the synthesis of oxygen substoichiometric samples. Iodometric titration method has been applied to determine the average state valence of cobalt species. The end-point is electrochemically determinated by following the potential of the solution with platinum electrodes versus ECS electrode, while the current is held at zero. Each sample (ca. 50 mg) is dissolved in a molar acetic buffer solution (ca. 50 mL) containing an excess of KI (ca. 1 g). Co(+III) and Co(+IV) species are reduced into Co(+II) together with formation of iodine species in stoichiometric amount. Iodine is therefore titrated with $Na_2S_2O_3$ 0.1 N solution using thiodene (starch) as colorimetric indicator in addition to the potential evolution.

3. Results and discussion

3.1. Crystal chemistry

The X-ray powder diffraction (XRPD) patterns, collected by using an X-pert Pro diffractometer equipped with X'Celerator detector and working with Cu$K\alpha$ radiation ($5° \leqslant 2\theta \leqslant 140°$, 0.0167° step), have revealed that for the low nominal amount of cerium, typically $x < 0.2$, $Sr_6Co_5O_{15}$ phase is systematically detected as secondary phase. In contrast, for $x \approx 0.25$ a nearly pure phase is obtained since the whole pattern can be indexed in the I-type lattice with $a_p \times a_p \times 20$ Å^3 cell parameters—where a_p is the perovskite cell parameter—with only few traces of $Sr_6Co_5O_{15}$ as impurity (asterix in Fig. 1). If no significant splitting of peaks at high angles has been detected, an FWHM broadening of (h0l) peaks is observed (Fig. 1c) characteristic of a slight orthorhombic distorsion. For larger amounts of cerium, typically $x \geqslant 0.3$, traces of (Sr,Ce)$CoO_{3-\delta}$ perovskite and CeO_2 oxide were found. To check further the crystallographic quality, the compound $Sr_{2.75}Ce_{0.25}Co_2O_{7-\delta}$ has also been studied by transmission electron microscopy (JEOL 2010CX electron microscope). The electron diffraction patterns (Fig. 2) are consistent with the I-type symmetry ($a \sim 3.8$ Å and $c \sim 20$ Å) but they evidence extra diffuse lines (white arrows in Fig. 2b) parallel to c^*-axis. This structural feature is often observed in the deficient RP-type structures and lead to a superstructure and lower symmetry [12]. The corresponding [100] HREM image is showed in Fig. 2c in which low electron density zones are correlated to white dots. In the present case, the diffuse lines can be ascribed to a disorder between oxygen and vacancy sites at the level of perovskite block (white arrows in Fig. 2c). The coupled energy dispersive spectroscopy (EDS) analyses have confirmed that the cation contents of the microcrystals, "$Sr_{2.75}Ce_{0.25}Co_2$" are almost unchanged in comparison to the starting composition. An average cobalt oxidation state $V_{Co} = +2.62$, assuming Ce^{4+} species is deduced from the iodometric titrations which leads to an oxygen content corresponding to $O_{5.87(5)}$. Note that in the case of this Ce doped RP2 cobaltate, no reactivity in air is observed in opposite to the oxygen deficient undoped $Sr_3Co_2O_6$ phase [11,12]. A post-annealing treatment in an oxygen pressure (300 °C, 100 atm, 12 h) has been also made to try to fill the oxygen vacancies. A weight gain of about 3% is observed in agreement with the new oxygen stoichiometry of this "PO_2" sample that is found to be $O_{6.77(5)}$ ($V_{Co} = +3.52$) from iodometric titrations. This oxygen uptake impacts the microstructure since the electron diffraction study gives in evidence a tetragonal RP2-type lattice ($a_p \times a_p \times 20$ Å^3) without the extra diffuse lines along c^* firstly observed in the case of the "as-prepared" (Fig. 2b).

3.2. Rietveld analyses

In order to limit the parameters and follow the cell parameters evolution, the Rietveld analyses have been performed with the same $I4/mmm$ space group. These structural refinements from XRPD data (Fig. 1) for the "as-prepared" and "PO_2" $Sr_{2.75}Ce_{0.25}Co_2O_{7-\delta}$ samples indicate that the unit-cell parameters decrease, as the oxygen content increases, from $a = b = 3.836$ Å, $c = 20.453$ Å to $a = b = 3.815$ Å and $c = 20.047$ Å for the "as-prep." and "PO_2" samples, respectively, in agreement with the smaller ionic radius for the more oxidized cobalt cations. The too low cerium content does not allow to detect a preferential occupation over the two possible sites, in the perovskite block or at the level of the rock salt layer, respectively. Additionally, even if XRPD are not suitable to quantify the actual oxygen content, the occupation factors revealed vacancies on the O(1) and O(3) sites for the as-prepared sample (Fig. 3b). These sites were occupied at 75% and 91%, respectively, while the BVS (bond valence state) calculations using the SoftBV software [18] and the Co–O distances listed in Table 2 lead to 2.68+ and 2.56+ considering $R_0(Co^{2+})$ and $R_0(Co^{3+})$, respectively. These results lead to a total oxygen content of 5.9, in close

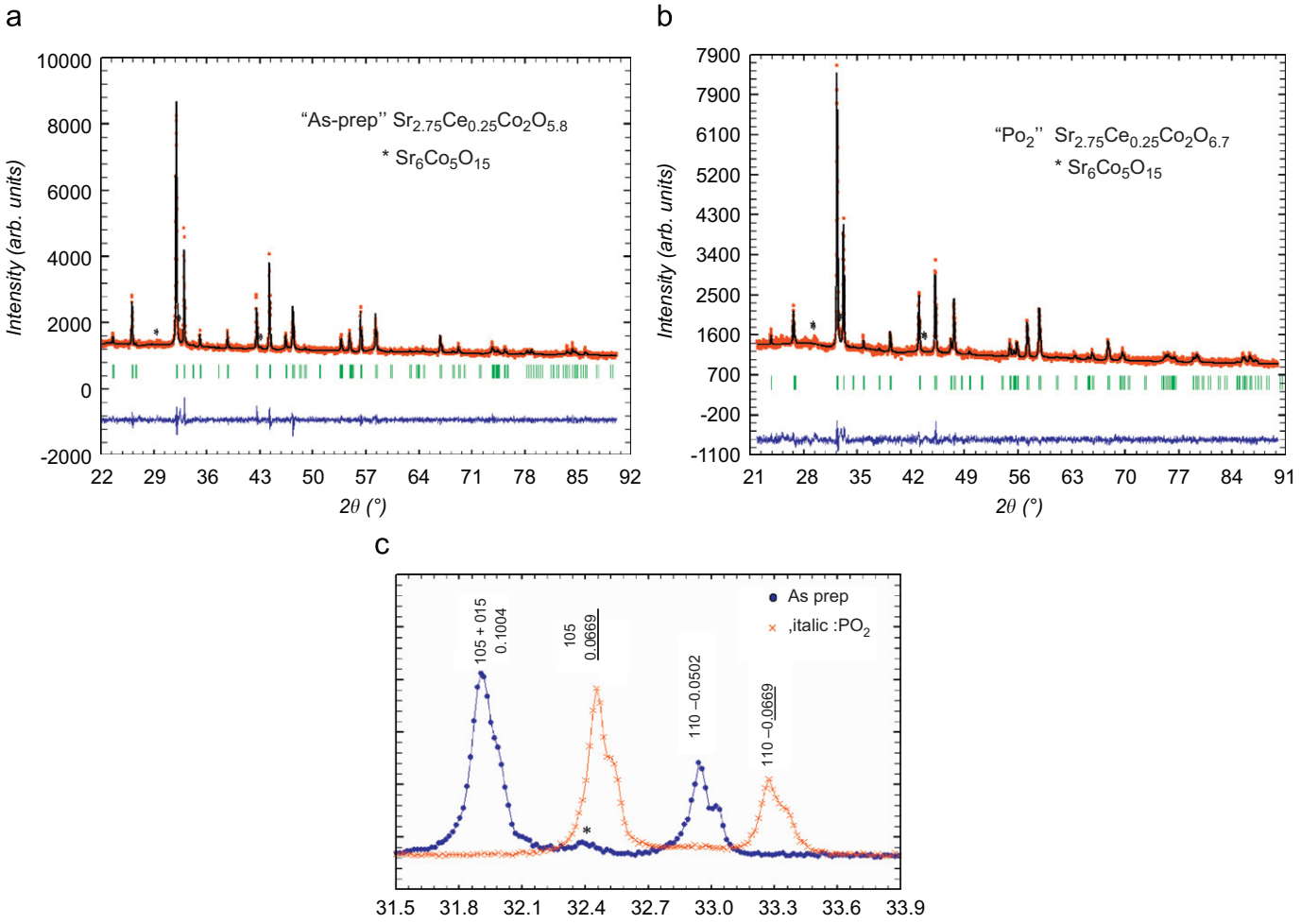

Fig. 1. X-ray powder diffraction (XRPD) patterns of the (a) as-prepared and (b) oxygen pressure (100 bar) annealed phases $Sr_{2.75}Ce_{0.25}Co_2O_{7-\delta}$.The two experimental patterns are indexed (vertical bars) in the $I4/mmm$ tetragonal ($a_p \times a_p \times 20$ Å^3) lattice. An enlarged part of patterns is shown in (c) to illustrate the shifting of cell parameters and the broadening of (105) peak in the as-prepared $Sr_{2.75}Ce_{0.25}Co_2O_{5.9}$ sample.

agreement with that obtained from iodometric titration. Note that the orthorhombic *Immm* setting has been also considered in agreement with the FWHM (h0l) broadening (Fig. 1c) observed in the case of the as-prepared sample. Even if a slight orthorhombic distortion is revealed by the refined values of a and b cell parameters, $a = 3.8344(1)$ Å and $b = 3.8410(2)$ Å, respectively, no significant decrease of reliability factors is observed except for the χ^2 that decreases from 5.25 to 4.69. In this setting, the refinements of occupation factors lead to a whole oxygen stoichiometry close to 5.92 with an occupation site of both oxygen sitting in cobalt layers of 78% and 68%, respectively. This result agrees with the 56% and 52% occupations of the equivalent oxygen sites (sites O(1), O(3) and O(4) in Fig. 3a) reported for the deficient $Sr_3Co_2O_{5.64}$ oxides [10]. In the latter study based from neutron data, the oxygen atoms forming the theoretical CoO_4 planes are distributed on two distinct sites, O(1) and O(4), respectively. One is fully occupied and the second one is deficient with 56% occupation (Fig. 3a). Such a distribution is responsible for the large orthorhombic distortion of the lattice, clearly observed from X-ray diffraction data [10,11]. In contrast, our compounds exhibit a pseudo-tetragonal lattice without a specific filling of oxygen sites in cobalt layers. This structural difference highlights the role played by the cerium cation in stabilizing a different symmetry linked to a different distribution of the oxygen vacancies. The two models are compared in Fig. 3. The refinements of the PO_2 annealed sample converge on a nearly fully oxygenated structure with a slight oxygen deficiency (~6%) only at the level of the cobalt layers (O(1) site in Fig. 3b). The resulting oxygen stoichiometry is close to "$O_{6.7}$" in agreement with the analysis by iodometric titration and the weight gain. Some BVS calculations have been also carried out (see Table 2). The obtained values must be interpreted cautiously since the $R_0(Co^{4+})$ is not perfectly tabulated. However, a simple average calculation from both values leads to a 3.64+ value for cobalt state valence.

The final Rietveld refinements carried out with the tetragonal $I4/mmm$ setting and the main atomic distances including BVS results are summarized in Tables 1 and 2, respectively.

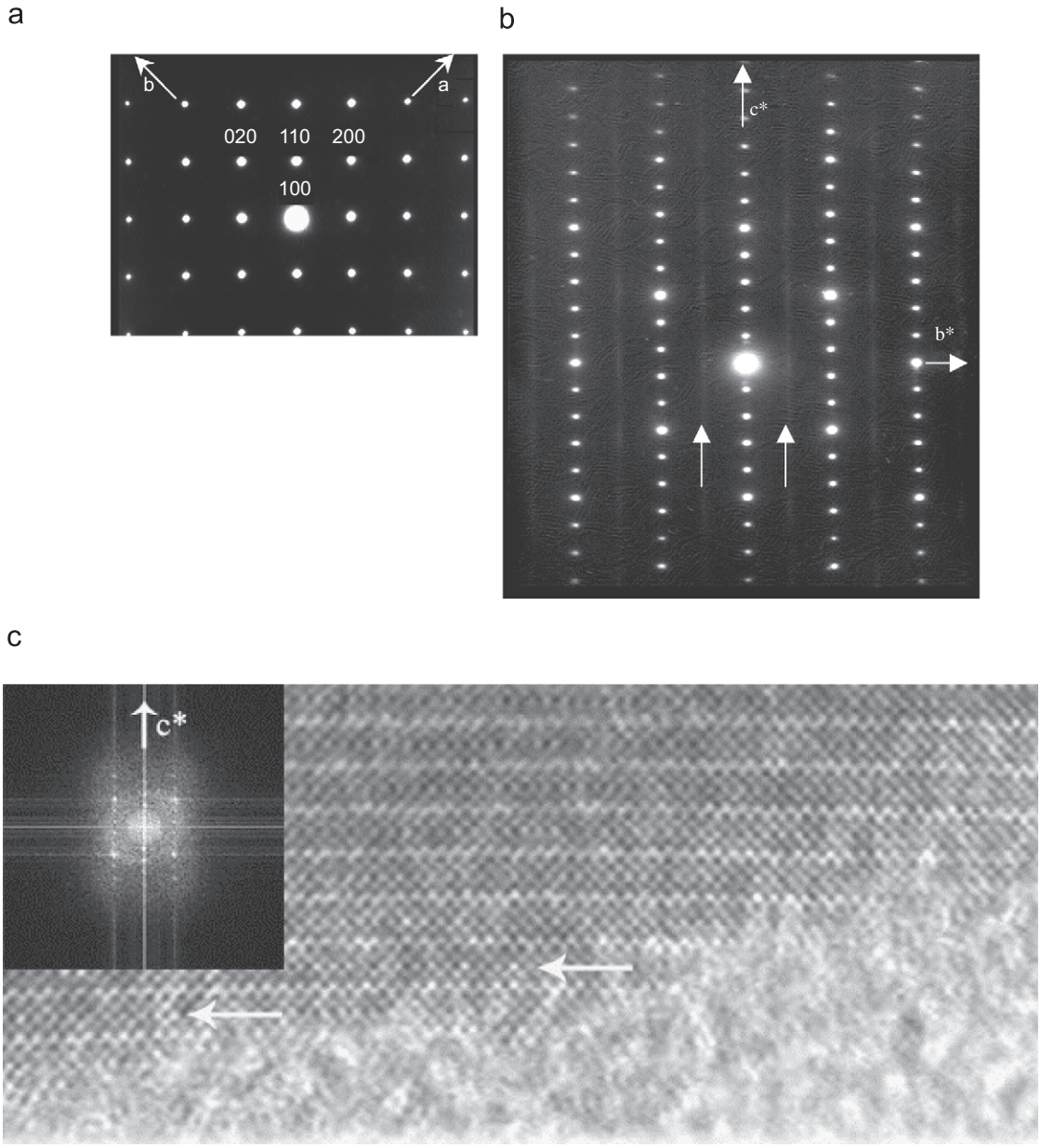

Fig. 2. Experimental electron diffraction of as-prepared $Sr_{2.75}Ce_{0.25}Co_2O_{5.9}$: (a) [001] and (b) [100] oriented patterns. Diffuse lines are pointed by white arrows. The corresponding [100] HREM image recorded at Scherzer value ($\Delta f \approx -250$ Å) is shown in (c).

3.3. Magnetic and transport features

The possibility to stabilize and then oxidize by post-annealing this $n=2$ RP cobaltate creates a unique opportunity to study the magnetic (SQUID magnetometry) and transport properties (four-probe resistivity). The "as-prepared" $Sr_{2.75}Ce_{0.25}Co_2O_{5.9}$ sample exhibits a very weak magnetism (Fig. 4a) associated with a semi-conducting state with $\rho_{300\,K} \sim 2 \times 10^3\,\Omega$ cm (Fig. 5) and an activation energy of 260 meV. From the Curie–Weiss fitting to the $\chi^{-1}(T)$ curve (Fig. 4b) performed between 50 and 175 K, one obtains $\theta_{cw} = -310$ K indicating dominating antiferromagnetic interactions in the paramagnetic state. This fitting yields an effective paramagnetic moment $\mu_{eff} = 3.3\mu_B$/Co. From the chemical formula giving $V_{Co} \sim +2.65$ one could expect a mixture of high spin Co^{2+} ($S = \frac{3}{2}$, $\mu_{eff} = 3.9\mu_B$) and Co^{3+} but with different possible spin states for the latter (high spin, $S = 2$, $\mu_{eff} = 4.9\mu_B$; intermediate spin, $S = 1$, $\mu_{eff} = 2.83\mu_B$; low spin, $S = 0$, $\mu_{eff} = 0$). This prevents any serious conclusion to be drawn from the μ_{eff} value. Nonetheless, the comparison with the data for the "PO_2" sample, $Sr_{2.75}Ce_{0.25}Co_2O_{6.7}$, are very instructive. The $\chi(T)$ curves, collected in zero field cooling (zfc) and field cooling (fc) mode within 0.3 T, reveal the development of a large ferromagnetic component below $T_C \sim 175$ K which confirms the dramatic change of the magnetic ground state induced by the oxygen uptake (Fig. 4a). The strong irreversibility below the zfc and fc curves strongly suggests the existence of coercive field larger than 0.3 T which is confirmed by the isothermal

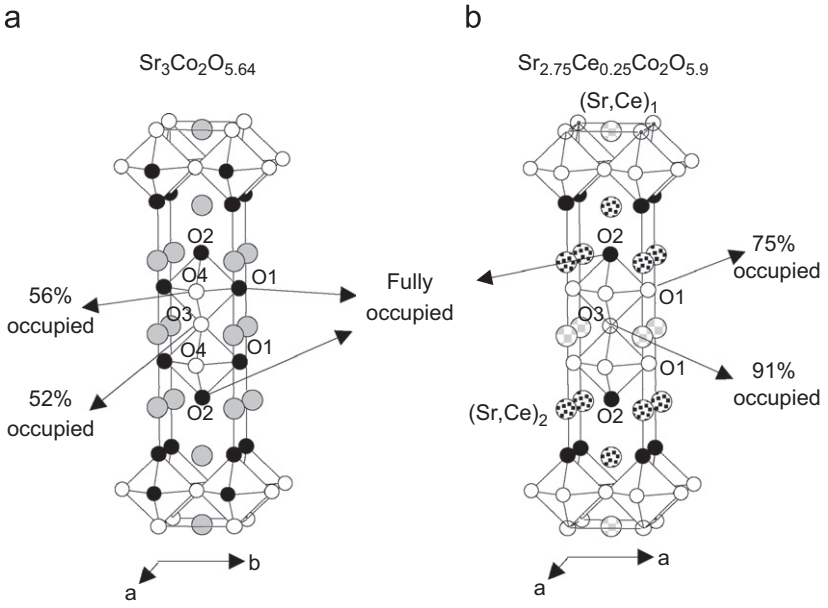

Fig. 3. Structural model of oxygen deficient RP2 (a) $Sr_3Co_2O_{5.64}$ (from Ref. [19]) and (b) $Sr_{2.75}Ce_{0.25}Co_2O_{5.9}$ phases. Oxygen sites are labeled with black filled and checkerboard circles depending on fully or partially filling, respectively.

Table 1
Refined atomic positions

	"As prep" $Sr_{2.75}Ce_{0.25}Co_2O_{5.9}$						*"PO_2" $Sr_{2.75}Ce_{0.25}Co_2O_{6.7}$*					
Atom	Site	Occupancy	x	y	z	B (Å^2)	Site	Occupancy	x	y	z	B (Å^2)
(Sr/Ce)1	2*b*	(0.92/0.08)	0	0	1/2	0.9(2)	2*b*	(0.92/0.08)	0	0	1/2	1.0(2)
(Sr/Ce)2	4*e*	(0.92/0.08)	0	0	0.3159(2)	1.5(2)	4*e*	(0.92/0.08)	0	0	0.3168(2)	1.3(2)
Co	4*e*	1	0	0	0.0989(3)	1.8(2)	4*e*	1	0	0	0.0976(4)	1.8(2)
O1	8*g*	0.75(8)	0	1/2	0.086(1)	1.0[a]	8*g*	0.94(2)	0	1/2	0.0926(9)	1.0[a]
O2	4*e*	1	0	0	0.1967(8)	1.0[a]	4*e*	1	0	0	0.1945(9)	1.0[a]
O3	2*a*	0.91(6)	0	0	0	1.0[a]	2*a*	1	0	0	0	1.0[a]
*I*4/*mmm*							*I*4/*mmm*					
$a = 3.8364(1)$ Å							$a = 3.8148(1)$ Å					
$c = 20.4527(7)$ Å							$c = 20.0466(4)$ Å					
$R_B = 8.45$ $\chi^2 = 5.25$							$R_B = 8.98$ $\chi^2 = 4.82$					

[a]Not refined.

Table 2
Main atomic distances

"As prep" $Sr_{2.75}Ce_{0.25}Co_2O_{59}$		"PO_2" $Sr_{2.75}Ce_{0.25}Co_2O_{6.7}$	
(Sr/Ce)1–O1 × 8[a]	2.600(1) Å	(Sr/Ce)1–O1 × 8[a]	2.660(1) Å
–O3 × 4[a]	2.713(1) Å	–O3 × 4	2.697(1) Å
(Sr/Ce)2–O1 × 4[a]	2.77(1) Å	(Sr/Ce)2–O1 × 4[a]	2.63(1) Å
–O2 × 1	2.46(2) Å	–O2 × 1	2.45(2) Å
–O2 × 4	2.725(1) Å	–O2 × 4	2.707(2) Å
Co–O1 × 4[a]	1.939(2) Å	Co–O1 × 4[a]	1.910(1) Å
–O2 × 1	2.00(2) Å	–O2 × 1	1.94(2) Å
–O3 × 1[a]	2.023(6) Å	–O3 × 1	1.960(6) Å
BVS = +2.56 assuming $R_0(Co^{3+})$		BVS = +2.80 assuming $R_0(Co^{3+})$	
BVS = +2.68 assuming $R_0(Co^{2+})$		BVS = +4.48 assuming $R_0(Co^{4+})$	

[a]Partially occupied.

magnetic field dependence of the magnetization (M) (Fig. 4c) showing $\mu_o H_C = 1$ T and a saturation almost reached in 5 T with $M_{5T} \approx 0.8\mu_B$/Co. This ferromagnetic behavior, recently reported for the phase $Sr_3Co_2O_{6.60}$ [19], goes with a change of the μ_{eff} value. The latter, deduced from the χ^{-1} (T) fitting in the range from 200 to 300 K (Fig. 4b), increases from $\mu_{eff} = 3.3$ to $4.2\mu_B$/Co as the oxygen content increases from $O_{5.9}$ to $O_{6.7}$. For the latter, it corresponds to $V_{Co} \sim +3.5$, so that the experimental value of $\mu_{eff} = 4.2\mu_B$/Co cannot be explained by a mixture of IS Co^{3+} ($S = 1$)/Co^{4+} ($S = 3/2$) yielding to $\mu_{eff} = 3.3\mu_B$/Co. This suggests that higher spin states for Co^{3+} and/or Co^{4+} species. Nevertheless, the existence of ferromagnetism can be interpreted by a kind of double-exchange mechanism in the case of the "PO_2" sample showing a much more conducting behavior than the "as-prepared" sample

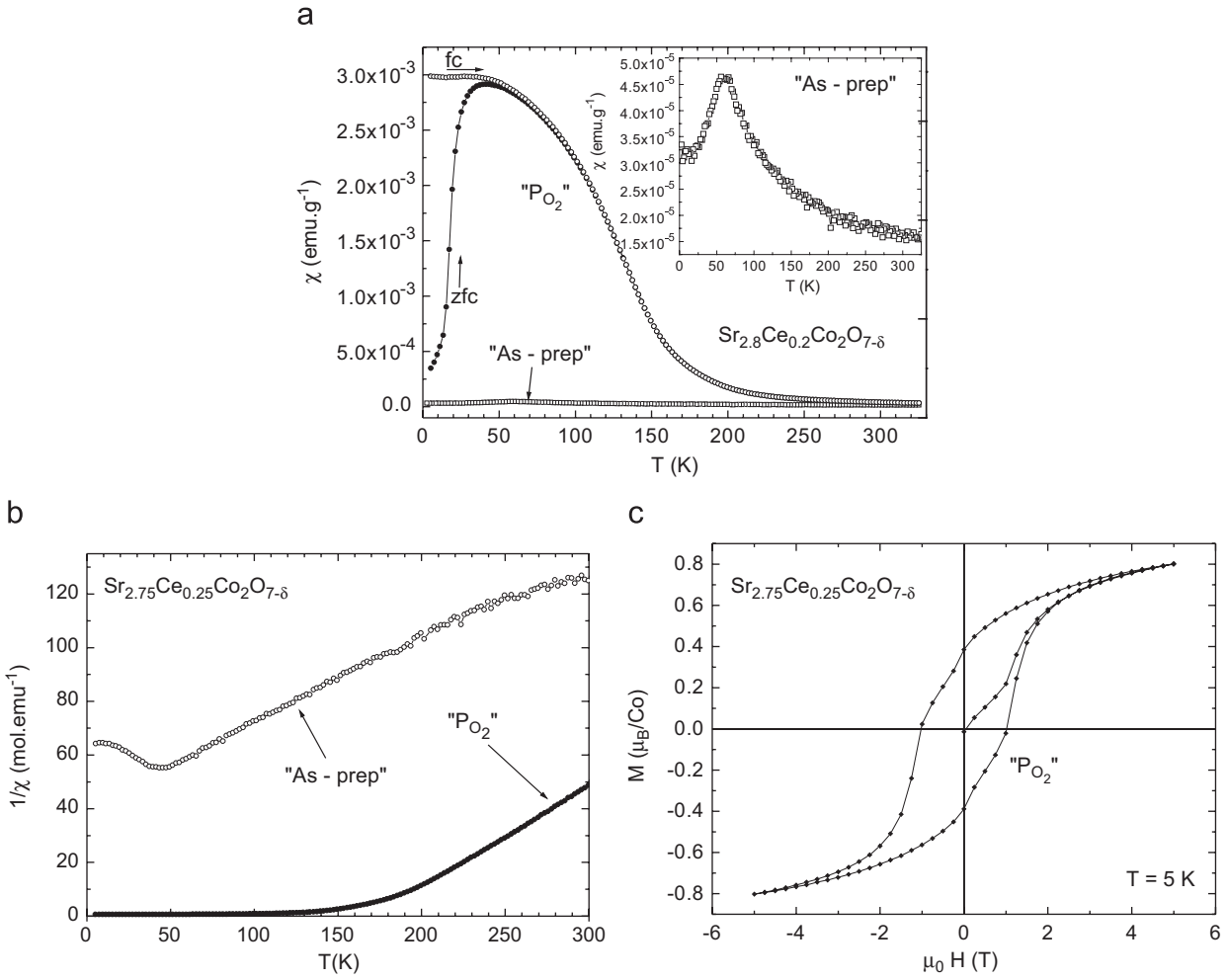

Fig. 4. (a) T dependence of the magnetic susceptibility (χ) "as-prepared" (enlarged curve in insert) and "PO_2" $Sr_{2.75}Ce_{0.25}Co_2O_{7-\delta}$ .The data are collected in 0.3 T. The zfc and fc are for zero field cooling and field cooling process. (b) $\chi^{-1}(T)$ corresponding curves. (c) Isothermal ($T = 5$ K) $M(H)$ curve for the post-annealed $Sr_{2.75}Ce_{0.25}Co_2O_{7-\delta}$.

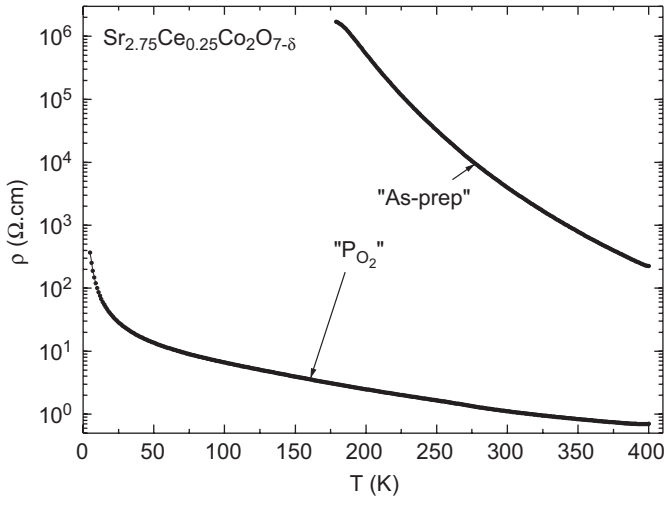

Fig. 5. T-dependent resistivity (ρ) of the "as-prepared" and "PO_2" phases $Sr_{2.75}Ce_{0.25}Co_2O_{7-\delta}$. The $\rho(T^{-1})$ data are also given (top x-axis).

involving a charge delocalization in the e_g bands as the core spins in the t_{2g} bands are ferromagnetically coupled. This is corroborated by the $\rho(T)$ curve showing a much lower resistivity, $\rho_{300\,K} = 1\,\Omega$ cm for $O_{6.7}$ against $\rho_{300\,K} \sim 10^3\,\Omega$ cm for $O_{5.9}$, and also a much less activated behavior for the former (Fig. 5). At high T, in the paramagnetic regime ($T > 200$ K), the $\rho(T)$ curve can be fitted using a semiconducting behavior, with an activation energy of 50 meV, to be compared to 260 meV for the as-prepared sample. At lower T, below the magnetic transition temperature, the activation energy decreases. This more conducting state associated with the ferromagnetic state is also sensitive to application of an external magnetic field (Fig. 6) leading to a negative magnetoresistance [$MR = 100 \times (\rho_{7\,T} - \rho_{0\,T})/\rho_{0\,T}$] reaching at 15 K $MR = -4\%$, a value comparable to those reported for the ferromagnetic metallic perovskites $SrCoO_{3-\delta}$ [7].

4. Conclusions

In conclusion, it has been shown that a small amount of cerium substituted for strontium favors the stabilization of the $n = 2$ RP phase, $Sr_{2.75}Ce_{0.25}Co_2O_{7-\delta}$ with an oxygen deficiency which can be reduced by oxidizing post-annealing treatment from $\delta \approx 1.1$ ("as-prepared") to

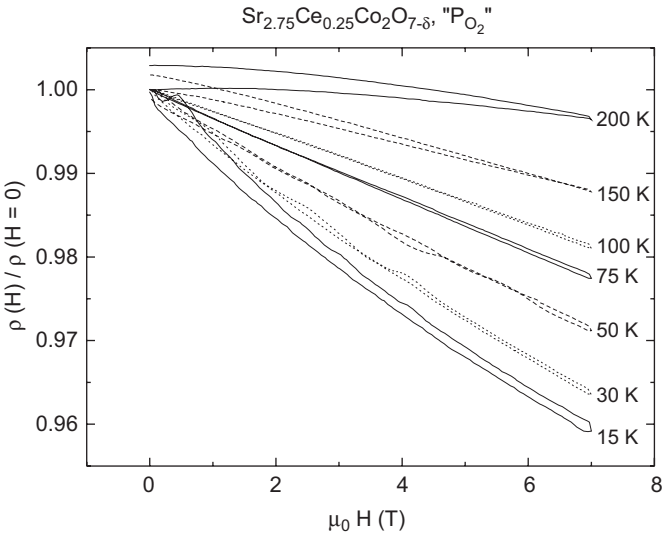

Fig. 6. Isothermal magnetic field dependence of the resistivity for the "PO_2" sample $Sr_{2.75}Ce_{0.25}Co_2O_{7-\delta}$.

$\delta \approx 0.3$ ("PO_2"). The main effect of this substitution on the structure concerns the *pseudo*-tetragonal symmetry of the unit-cell instead of the marked orthorhombic symmetry reported for the oxygen deficient analogues $Sr_3Co_2O_{6-\delta}$. Such a tetragonal $I4/mmm$ space group was also reported in the $n = 2$ RP phases $Sr_2Y_{1-x}Ca_xCo_2O_6$ [20,21] for which the $Y_{1-x}Ca_x$ central layer of the perovskite block favors the formation of a double row of tetragonal space square pyramids. In the present case of cerium substitution for strontium, the oxygen vacancies tend also to be located at the double perovskite block but on two distinct sites: at the level of square CoO_2 planes (O(1) site) and at the level of the common apical oxygen O(3) site with the two perovskite blocks. The distribution of oxygen vacancies in the square planes of the CoO_x polyhedra is thus in marked contrast with the ordering of the oxygen vacancies in that plane for the compounds $Sr_3Co_2O_{7-\delta}$ explaining the orthorhombic distortion of the latter for $\delta < 1$. Accordingly, this structural difference, concerning the location of the oxygen vacancies, creates different kinds of CoO_x polyhedra for $Sr_{2.75}Ce_{0.25}Co_2O_{7-\delta}$ and $Sr_3Co_2O_{7-\delta}$. In particular, the CoO_4 tetrahedra for the latter ($\delta \sim 1$ in Ref. [10]), appear to be responsible for their reactivity in air at room temperature transforming them into the corresponding oxyhydrates [12].

Interestingly, the compound $Sr_{2.75}Ce_{0.25}Co_2O_{7-\delta}$, when sufficiently oxidized, such as $\delta \sim 0.3$, becomes ferromagnetic with a much more conducting behavior as compared to its reduced counterpart ($\delta \sim 1.1$). This result is in good agreement with the results obtained for the $n = 1$ and ∞ RP members showing strong ferromagnetism for Sr_2CoO_4 [8] and $SrCoO_3$ [7].

Finally, these results also confirm the ability of cerium to be substituted in RP strontium based cobaltates after the reports for $n = \infty$ [9,15] and $n = 1$ [16] phases. An extended work is now necessary to find a chemical technique to completely fill the oxygen vacancies in order to reach a full oxygen stoichiometry. This would reinforce the ferromagnetism and thus allow to enhance the Curie temperature of the present $n = 2$ RP phase limited to $T_C = 175\,K$ for $Sr_{2.75}Ce_{0.25}Co_2O_{6.7}$ against $T_C \approx 270$–$280\,K$ for $SrCoO_3$ and Sr_2CoO_4.

Acknowledgement

The authors are grateful to Dr V. Pralong for the discussions about the iodometric titration controlled by electrochemical techniques.

References

[1] S. Yamaguchi, H. Taniguchi, H. Takagi, T. Arima, Y. Tokura, J. Phys. Soc. Jpn. 64 (1995) 1885.
[2] I. Terasaki, Y. Sasago, K. Uchinokura, Phys. Rev. B 56 (1997) R12685.
[3] A.V. Kovalevsky, V.V. Kharton, E.N. Naumovich, Russ. J. Electrochem. 33 (2) (1997) 170.
[4] K. Takada, H. Sakurai, E. Takyama-Mutomachi, F. Izumi, R.A. Dilanmian, T. Sasaki, Nature 422 (2003) 53.
[5] A. Maignan, V. Hardy, S. Hébert, M. Drillon, M.R. Lees, O. Petrenko, D. Mc K. Paul, D. Khomskii, J. Mater. Chem. 14 (2004) 1231.
[6] A. Maignan, V. Caignaert, B. Raveau, D. Khomskii, G. Sawatzky, Phys. Rev. Lett. 93 (2004) 026401.
[7] P. Bezdicka, A. Wattiaux, J.C. Grenier, M. Pouchard, P. Hagermuller, Z. Anorg. Allg. Chem. 619 (1993) 7.
[8] J. Matsuno, Y. Okimoto, Z. Fang, X.Z. Yu, Y. Matsui, N. Nagaosa, M. Kawasaki, Y. Tokura, Phys. Rev. Lett. 93 (2004) 167202.
[9] S. Hébert, A. Maignan, V. Caignaert, V. Pralong, D. Pelloquin, B. Raveau, Solid State Commun. 134 (2005) 815.
[10] L. Viciu, H.W. Zandbergen, Q. Xu, Q. Huang, M. Lee, R.J. Cava, J. Solid State Chem. 179 (2006) 5010.
[11] S.E. Dann, T.M. Weller, J. Solid State Chem. 115 (1995) 499.
[12] D. Pelloquin, N. Barrier, A. Maignan, V. Caignaert, Solid State Sci. 7 (2005) 853.
[13] S.Y. Istomin, O.A. Drozhin, G. Svensson, E.V. Antipov, Solid State Sci. 6 (2004) 539.
[14] R.L. Withers, M. James, D.J. Goossens, J. Solid State Chem. 174 (2003) 198.
[15] N.E. Trofinenko, J. Paulsen, H. Ullmann, R. Müller, Solid State Ionics 100 (1997) 183.
[16] M. James, K.S. Wallwork, R.L. Withers, D.J. Goossens, K.F. Wilson, J. Horval, Y.L. Wang, M. Colella, Mater. Res. Bull. 40 (2005) 1415.
[17] A. Maignan, B. Raveau, S. Hébert, V. Pralong, V. Caignaert, D. Pelloquin, J. Phys. Condens. Matter 18 (2006) 4305.
[18] S. Adams, Acta Cryst. B 57 (2001) 278–287 SoftBV software.
[19] J.M. Hill, B. Dabrowski, J.F. Mitchell, J.D. Jorgensen, Phys. Rev. B 74 (2006) 174417.
[20] K. Yamaura, Q. Huang, R.J. Cava, J. Solid State Chem. 146 (1999) 277.
[21] K. Yamaura, D.P. Young, R.J. Cava, Phys. Rev. B 63 (2001) 064401.